MODELLING LINEAR COUPLING FOR FCC-ee IN XSUITE

V. Gawas*[1], F. Zimmermann, X. Buffat, R. Tomás Garcia
CERN, European Organization for Nuclear Research, Geneva, Switzerland
[1]University of Geneva, Geneva, Switzerland †

Abstract

Accurate control of transverse linear coupling is important for achieving the target luminosity in FCC-ee. We have implemented a simplified FCC-ee coupling model in Xsuite based on linear maps and the Edwards-Teng formalism. This approach is benchmarked against the full FCC-ee optics model, showing good agreement in betatron tunes, beta functions, and coupling-related quantities. The coupling matrix elements are derived as a function of resonance driving terms (RDTs) and validated against analytical calculations of f_{1001} and f_{1010}. The coupled model is then used in strong-strong beam-beam simulations to study the impact of controlled RDT excitations on luminosity, beam size, emittance, and beamstrahlung power at the ZH and $t\bar{t}$ operating points. This work presents a practical framework for coupling studies and provides a basis for developing FCC-ee coupling tolerances and luminosity tuning procedures.

INTRODUCTION

Linear coupling between the horizontal and vertical betatron motion plays a critical role in determining the achievable beam sizes and luminosity in the FCC-ee collider [1]. In the interaction regions (IRs), coupling arises primarily from detector solenoids, anti- and shielding solenoids, quadrupole magnet roll errors, and sextupole magnet misalignments. Even weak coupling can lead to vertical emittance growth, tune splitting, and beam-size blow-up at the interaction point (IP), thereby degrading luminosity and changing beamstrahlung emission.

Beam-beam simulations carried out for assessing the luminosity performance often rely on simplified lattice models, in which the detailed machine optics is replaced by compact linear transport maps combined with a beam-beam element at the interaction point (IP) [2]. For accurately capturing the impact of coupling in such models, a consistent representation of linear coupling is required. To accomplish this, we have implemented a coupled linear transport model in the code Xsuite [3]. Our model is based on the Edwards-Teng formalism [4], which expresses the coupled betatron motion in terms of two normal modes. The transport from the crab sextupoles to the IP is represented by a factorized map consisting of uncoupled normal-mode motion and local coupling matrices at the start and end points.

The model parameters are extracted from a Twiss analysis of the full FCC-ee lattice, including possible skew quadrupole excitations. The complete lattice based on linear transport maps is validated against the full nonlinear lattice of the FCC-ee by comparing linear optics observables such as tunes and IP β-functions.

Our ring model with a single IP comprises an upstream crab sextupole, a coupled transport matrix to that IP, a beam-beam element, the inverse transport to the downstream crab sextupole, and an arc section including radiation damping and quantum excitation. This model can be used combined with strong-strong beam-beam simulations at the IP, to explore the impact of deliberately introduced local IP coupling on luminosity, beam sizes, emittance, and beamstrahlung at different operating energies of the collider.

COUPLED TRANSPORT IN XSUITE

The 4×4 coupled transport between two locations can be written in the Edwards-Teng form as [4]

$$M_{12} = V_{s2} \begin{pmatrix} A_{12} & 0 \\ 0 & B_{12} \end{pmatrix} V_{s1}^{-1} ,$$

where A_{12} and B_{12} are the Courant-Snyder matrices describing uncoupled motion of the two normal modes, and V_{s1}, V_{s2} contain the coupling information. The normal modes are obtained by diagonalizing the full coupled one-turn matrix. In the uncoupled normal-mode coordinates, the dynamics reduces to two independent harmonic oscillators with eigentunes Q_1 and Q_2.

Normal-Mode Optics Parameters

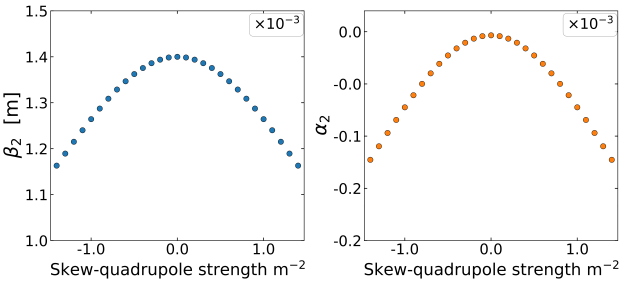

Figure 1: The IP normal mode functions β_2 and α_2 versus the strength of two skew quadrupoles (of opposite sign) inserted in the full lattice after the crab sextupoles on either side of the IP, in the absence of any beam-beam element.

The normal-mode Courant–Snyder matrices are fully determined by the Twiss parameters $\beta_{1,2}$, $\alpha_{1,2}$ and the phase advances of the two eigenmodes. In FCC-ee, the beams are extremely flat and the design tunes are not close to a linear coupling resonance, and after optics corrections the linear coupling is weak, so that the normal-mode optics functions remain close to those of the uncoupled optics. This simplifies the parameter extraction from a Twiss analysis of the

* vaibhavi.gawas@cern.ch
† This work was supported by the Swiss CHART programme.

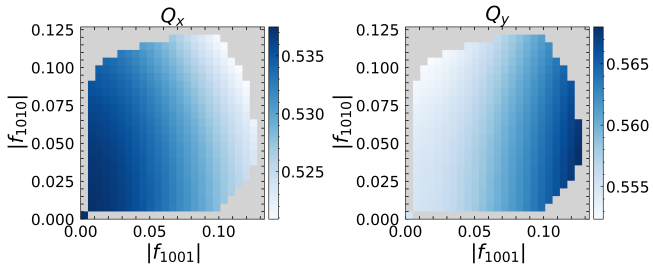

Figure 2: The change in eigentunes with increasing RDT values in linear lattice formalism.

full lattice with skew quadrupole excitations. Simulations reveal that the eigenmode β-functions and tunes only slightly change for realistic coupling strengths, justifying the use of nominal optics parameters in our simplified model. Figure 1 illustrates how the horizontal-mode functions β_1 and α_1 at the IP are perturbed by linear coupling.

The eigentune response to increasing coupling strength is shown in Fig. 2. For weak coupling, the eigentunes approximately satisfy $Q_1 + Q_2 \approx$ const. [5], with individual tunes shifting by only 0.015–0.020 over the RDT scan range. The difference resonance term f_{1001} dominates the tune splitting, while the sum resonance term f_{1010} plays a secondary role in the absence of beam-beam interactions.

Coupling Matrix Formalism

The local coupling in the transverse plane is encoded by the matrix V, which can be written as [6]

$$V = \begin{bmatrix} \gamma I & C \\ -C^+ & \gamma I \end{bmatrix}, \qquad \gamma = \sqrt{1 - \det C}, \tag{1}$$

where C is a 2×2 coupling matrix containing four independent parameters (and C^+ denotes its symplectic conjugate). The quantity γ determines the coupling strength and defines the Edwards–Teng coupling angle $\phi = \cos^{-1}\gamma$ [4, 7]. It is convenient to introduce a normalized coupling matrix $\bar{C}$ as

$$C = G_a^{-1}\bar{C}G_b, \qquad G = \begin{bmatrix} 1/\sqrt{\beta} & 0 \\ \alpha/\sqrt{\beta} & \sqrt{\beta} \end{bmatrix}, \tag{2}$$

which separates the intrinsic coupling strength in $\bar{C}$ from the local Twiss parameters [6].

In total, ten independent parameters are required to specify the coupled map: six describing the normal modes $(\alpha_{1,2}, \beta_{1,2}, Q_{1,2})$ and four describing the coupling matrix [7].

Relation to Linear Resonance Driving Terms

To link the coupling matrix formalism to measurable accelerator quantities, the normalized matrix elements can be written in terms of the RDTs as [8]

$$\begin{aligned} \bar{C}_{11} &= 2\gamma(\Im f_{1010} + \Im f_{1001}), \\ \bar{C}_{22} &= 2\gamma(\Im f_{1001} - \Im f_{1010}), \\ \bar{C}_{12} &= 2\gamma(\Re f_{1001} - \Re f_{1010}), \\ \bar{C}_{21} &= -2\gamma(\Re f_{1001} + \Re f_{1010}). \end{aligned}$$

The physical matrix elements follow by applying the transformation (2). This relation directly links RDT amplitudes to the coupling parameters in our model. Typical RDT values in FCC-ee lie in the range between 10^{-5} and 10^{-2}, according to lattice studies with realistic errors and corrections [1].

BEAM-BEAM WITH COUPLING

Strong-strong beam-beam simulations are performed using the coupled map model at the FCC-ee ZH and $t\bar{t}$ operating points [1]. Coupling is introduced in one beam only to isolate its effect, while the opposing beam remains uncoupled. This asymmetric configuration allows the independent contributions of the coupled and uncoupled beams to observables such as luminosity, beam size, and beamstrahlung power to be cleanly separated.

Luminosity Dependence

Figure 3 shows the luminosity as a function of $|f_{1001}|$ and $|f_{1010}|$ with full beam-beam interaction. The luminosity exhibits a substantially higher sensitivity to the sum resonance term f_{1010} than to the difference term f_{1001}, consistent with the known result that the sum resonance drives stronger instabilities in the weak-coupling regime [9–11]. The impact of coupling is also much more prominent at the $t\bar{t}$ than at the ZH working point. At the top energy threshold, an amplitude $|f_{1001}| \sim 5 \times 10^{-3}$ reduces luminosity by approximately 5%, while an equivalent drop is produced by $|f_{1010}| \sim 2 \times 10^{-3}$. At the Higgs energy, a 10% drop in luminosity is observed at an amplitude of $|f_{1001}| \sim 10^{-2}$, and about 15% from $|f_{1010}|$. The spread in the luminosity values at comparable RDT amplitudes corresponds to the difference in phase of the RDT and numerical noise of the macroparticle simulations.

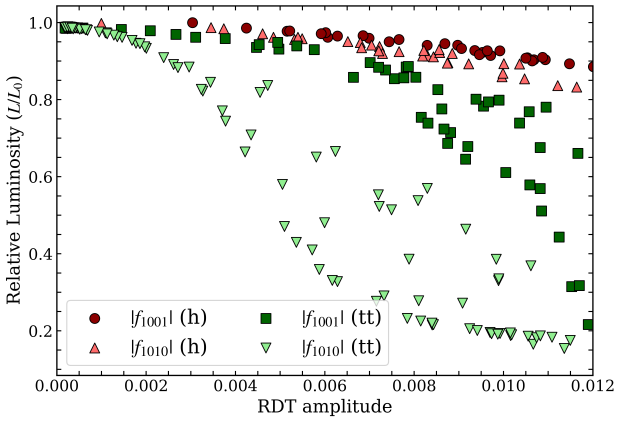

Figure 3: Luminosity dependence on $|f_{1001}|$ and $|f_{1010}|$ at ZH and $t\bar{t}$, with full beam beam. The luminosity was averaged over turns 800 to 1000 and normalized to the value at zero coupling.

The asymmetry is a direct consequence of the beam-beam tune shift. When the beam-beam strength is artificially reduced by nine orders of magnitude, the luminosity dependence becomes symmetric in the two RDTs as shown in Fig. 4, since without the beam-beam tune shift the bare

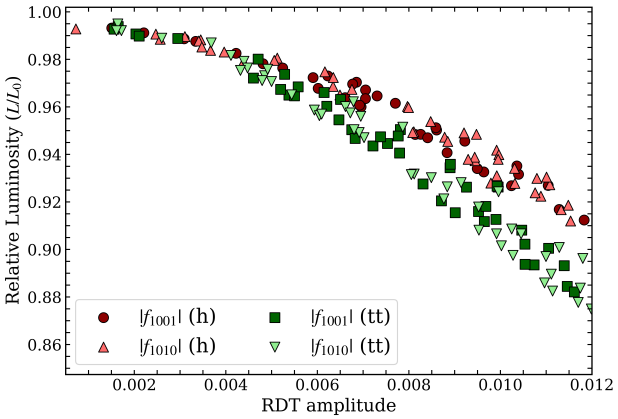

Figure 4: Luminosity dependence on $|f_{1001}|$ and $|f_{1010}|$ at $t\bar{t}$, with enormously (by a factor of 10^9) reduced beam-beam strength, the luminosity was averaged over turns 800 to 1000 and normalized to the value at zero coupling.

tunes sit much closer to the difference resonance, equalizing the relative drive of the two terms.

Beam Size, Emittance, and Bunch Length

Coupling increases the vertical beam size and vertical emittance of the coupled beam for both RDTs, with f_{1010} producing a markedly larger effect. At $|f_{\mathrm{RDT}}| \approx 5 \times 10^{-3}$, the vertical beam size grows by a factor of ~5 for f_{1001} and by ~20 for f_{1010} as shown in Fig. 5. The horizontal beam size is not significantly affected in either case. This vertical emittance blow-up is the primary mechanism behind the luminosity degradation described above.

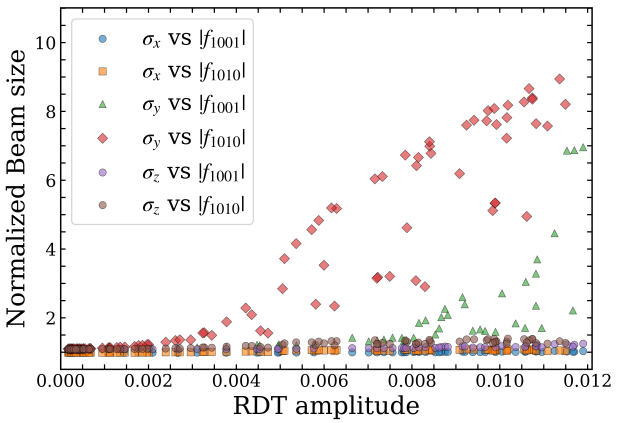

Figure 5: Normalized vertical and horizontal beam-sizes and bunch length vs. RDT amplitude at $t\bar{t}$.

The larger vertical beam size of the coupled beam reduces the beamstrahlung power emitted by the uncoupled beam, while the coupled beam itself radiates a correspondingly larger power, such that the total beamstrahlung power across both beams remains conserved as shown in Fig. 6. As a further consequence, the relatively smaller vertical emittance of the uncoupled beam leads to the bunch lengthening σ_z in the coupled beam by approximately 10% when beam-beam effects are active. Without beam-beam, the bunch length remains essentially unchanged, confirming that this effect

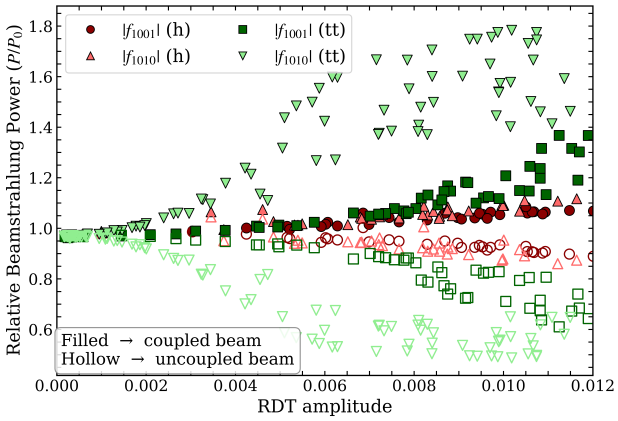

Figure 6: Normalized Beamstrahlung power of coupled and uncoupled beam vs. RDT amplitude at $t\bar{t}$ and ZH, averaged over turns 800 to 1000.

is driven by the interplay between coupling-induced emittance growth and beamstrahlung. The observation of beam size growth by a factor of four or more, accompanied by a strongly asymmetric beamstrahlung distribution between the two beams, indicates that the system has entered the flip-flop regime [12–14], in which the two beams settle into an asymmetric equilibrium with unequal emittances and beamstrahlung rates.

In a real machine with non-linear lattice constraints, even a beam-size blow-up at the level of about two times the nominal rms beam-size would already drive the system into a runaway regime. At such amplitudes, the beam is likely to encounter nonlinear resonances, leading to further emittance growth and loss of stability. If the coupling is not properly corrected, this process would ultimately result in particle losses at the mechanical aperture. Therefore , this sets a practical upper limit on the tolerable coupling strength, well below the highest values explored in the RDT scans presented here.

SUMMARY AND CONCLUSIONS

A coupled linear transport model for the FCC-ee interaction region accurately reproduces the optical effects of linear coupling observed in the full lattice, while providing a compact representation suitable for beam-beam simulations. Scans of the coupling strength expressed through RDTs reveal that, in the presence of the beam-beam interaction, the luminosity is particularly sensitive to the sum resonance term f_{1010}.

Adding coupling also increases the vertical beam size and emittance, and much more so in the presence of collisions, thereby impacting performance and operational tolerances. With beam-beam present, even the bunch length increases when adding coupling, as a side effect of beamstrahlung. The developed framework provides a practical tool for studying coupling effects in FCC-ee and will support future work on coupling correction, tuning strategies, and performance optimization across different operating modes.

REFERENCES

[1] "Future Circular Collider Feasibility Study Report Volume 2", *Eur. Phys. J. Spec. Top.*, vol. 234, no. 19, pp. 5713–6197, 2025. doi:10.17181/CERN.EBAY.7W4X

[2] P. Kicsiny, X. Buffat, G. Iadarola, T. Pieloni, D. Schulte, and M. Seidel, "Bhabha scattering model for multi-turn tracking simulations at the FCC-ee", in *Proc. IPAC'23*, Venice, Italy, pp. 682–685, Sep. 2023. doi:10.18429/JACoW-IPAC2023-MOPL062

[3] G. Iadarola *et al.*, "Xsuite: An Integrated Beam Physics Simulation Framework", in *Proc. HB'23*, Geneva, Switzerland, pp. 73–80, Mar. 2024. doi:10.18429/JACoW-HB2023-TUA2I1

[4] D. A. Edwards and L. C. Teng, "Parametrization of linear coupled motion in periodic systems", *IEEE Transactions on Nuclear Science*, vol. 20, no. 3, pp. 885–888, 1973. doi:10.1109/TNS.1973.4327279

[5] G. Parzen, "Theory of the tune shift due to linear coupling", *arXiv*, vol. 9910047, BNL-46415, 1999. https://arxiv.org/abs/physics/9910047

[6] D. Sagan and D. Rubin, "Linear analysis of coupled lattices", *Phys. Rev. Spec. Top. Accel. Beams*, vol. 2, no. 7, p. 074001, Jul. 1999. doi:10.1103/PhysRevSTAB.2.074001

[7] V. A. Lebedev and S. A. Bogacz, "Betatron motion with coupling of horizontal and vertical degrees of freedom*", *Journal of Instrumentation*, vol. 5, no. 10, P10010, Oct. 2010. doi:10.1088/1748-0221/5/10/P10010

[8] R. Calaga, R. Tomás, and A. Franchi, "Betatron coupling: Merging Hamiltonian and matrix approaches", *Phys. Rev. Spec. Top. Accel. Beams*, vol. 8, no. 3, p. 034001, Mar. 2005. doi:10.1103/PhysRevSTAB.8.034001

[9] DA. Edwards and MJ. Syphers, "An introduction to the physics of high energy accelerators". John Wiley & Sons, Ltd, 1993, pp. 144–171. doi:https://doi.org/10.1002/9783527617272.ch5

[10] H. Qin and R. C. Davidson, "Generalized Courant-Snyder theory for coupled transverse dynamics of charged particles in electromagnetic focusing lattices", *Phys. Rev. Spec. Top. Accel. Beams*, vol. 12, no. 6, p. 064001, Jun. 2009. doi:10.1103/PhysRevSTAB.12.064001

[11] P. N. Chirkov and I. I. Petrenko, "Sum Betatron Resonances under Linear Coupling of Oscillations", in *Proc. PAC'95*, Dallas, TX, USA, May 1995, paper FAB02, pp. 2792–2794.

[12] B. Richter, "The Stanford Positron - Electron Asymmetric Rings (SPEAR)", in *7th International Conference on High-Energy Accelerators*, vol. 2, pp. 81–93, Jul. 1969.

[13] M. H. R. Donald and J. M. Paterson, "An Investigation of the 'Flip-Flop' Beam-Beam Effect in SPEAR", in *Proc. PAC'79*, San Francisco, CA, USA, Mar. 1979, pp. 3580–3583.

[14] R. Holtzapple, F.-J. Decker, A. S. Fisher, and M. Sullivan, "Observation of Beam Size Flip-Flop in PEP-II", in *Proc. EPAC'02*, Paris, France, paper MOPRI011, pp. 410–412, Aug. 2007. https://jacow.org/e02/papers/MOPRI011.pdf